



The KMC-3 XPP beamline at BESSY II

Helmholtz-Zentrum Berlin für Materialien und Energie *

Instrument Scientists:

- Ivo Zizak, Helmholtz-Zentrum Berlin für Materialien und Energie
phone: +49 30 8062-12127, email: zizak@helmholtz-berlin.de

Abstract: The KMC-3 beamline is installed at the bending magnet of the BESSY II synchrotron light source. It provides a focused beam of monochromatic X-ray light at energies between 2.2 and 14 keV. It is dedicated to two experiments: X-ray Pump Probe (XPP) and CryoEXAFS.

1 Introduction

The XPP/KMC-3 is a middle range X-ray beamline providing monochromatic light between 2.2 and 14 keV for diffraction and absorption spectroscopy. Optionally the monochromator can be easily removed from the optical path providing a focussed white beam at the sample. Two permanent experiments mounted in the experimental hutch are dedicated to time-resolved x-ray diffraction and absorption spectroscopy experiments (EXAFS, XANES). In addition, the beamline equipment comprises an ultrafast laser as a pump source for time-resolved experiments.

2 Instrument Application

The KMC3 beamline is rather versatile and may be used for different experiments, including energy dispersive reflectometry and diffractometry. However, the main goal is to provide the monochromatic beam for time-resolved diffraction and absorption spectroscopy experiments. Typical experiments which can be performed at the beamline are mainly variations or combinations of the two permanent experiments mounted at the beamline: XPP-diffraction and CryoEXAFS.

2.1 X-ray Pump-Probe Diffraction

XPP experiment is run by the Joint Research Group between HZB and University Potsdam, Prof M. Bargheer. 80 cm diameter vacuum vessel is mounted around the focal spot of the last mirror. It encompasses a sample goniometer with a cryostat and slit/pinhole system to precisely tune the footprint

*Cite article as: Helmholtz-Zentrum Berlin für Materialien und Energie. (2017). The KMC-3 XPP beamline at BESSY II. *Journal of large-scale research facilities*, 3, A123. <http://dx.doi.org/10.17815/jlsrf-3-112>



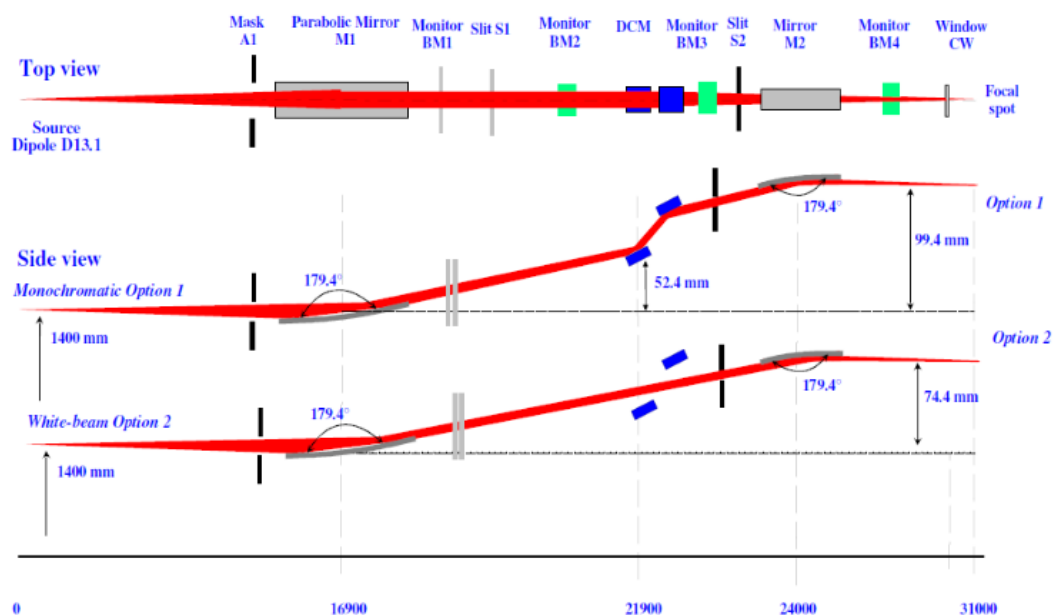


Figure 1: Optical layout of the KMC3 beamline.

at the sample. Pulsed laser beam is introduced into the beamline before the sample chamber, and can be focussed to the same spot at the sample. Different X-ray detectors are mounted outside of the vacuum and can be rotated up to scattering angle of 90° (Helmholtz-Zentrum Berlin für Materialien und Energie, 2016; Iurchuk et al., 2016; Navirian et al., 2014; Roshchupkin et al., 2016; Vadilonga et al., 2017).

2.2 CryoEXAFS

Cryo EXAFS is permanently mounted at mobile table, and can be connected to vacuum after the diffraction experiment. Having only several two Be windows in the optical path allows to perform EXAFS and XANES experiments down to K-line of Sulphur (experimentally not yet verified). However, measurements were already performed (not yet published) on Potassium K-edge (3.6 keV) and Ruthenium L3-edge (2.8 keV) using user-supplied experimental chambers.

Standard EXAFS experiment is mounted in vacuum (optionally He-atmosphere) and works in transmission and fluorescence geometry. The experiment is provided by the Cooperative Research Group of Prof. H. Dau, Free University Berlin (Görlin et al., 2016; Zaharieva et al., 2016).

3 Source

Source characteristics of the BESSY II dipole magnet 13.2 are summarized in the table 1.

4 Optical Design

The optical layout of the beamline is shown in figure 1. The bending magnet source D 13.1 is sagittally and meridionally collimated by the rotational paraboloid mirror M1. It is located at a distance of 16.9 m from the source. The double crystal (DCM) monochromator is located at a distance of 21.9 m from the source. Then the beam is refocused by the rotational paraboloid mirror M2 located at a distance of 24.0 m from the source (Fig. 1).

Electron energy	1.7 GeV
Magnetic field	1.3 T
Bending radius	4.35 m
Power (0.3 A, $3 \times 0.41 \text{ mrad}^2$)	50 W
Critical energy	2.5 keV
Source size (electron beam)	σ_x 0.15 mm σ_y 0.04 mm
Source divergence (electron beam)	σ'_x 388 μrad σ'_y 21 μrad

Table 1: Properties of the Dipole D 13.1 source.

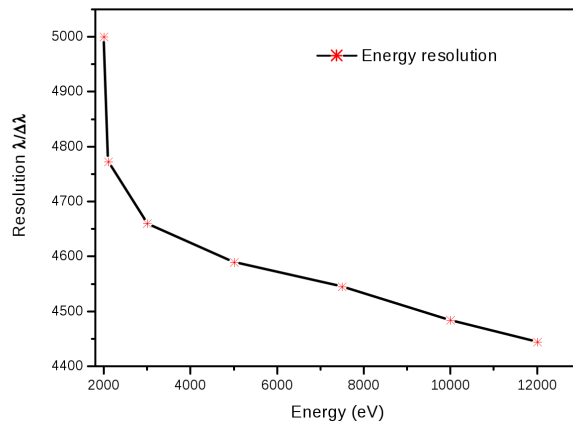


Figure 2: Energy bandwidth of the monochromatic beam.

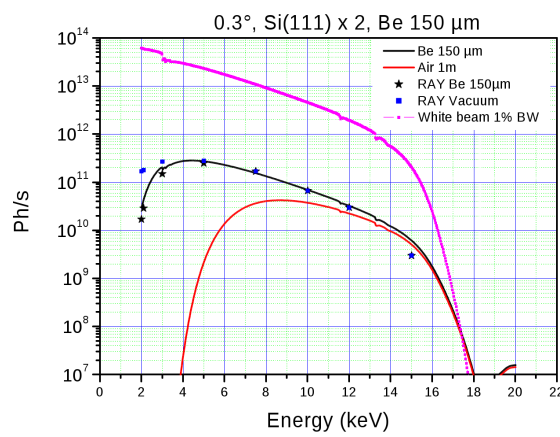


Figure 3: Comparison of the flux of the white and monochromatic beam in the focal spot.

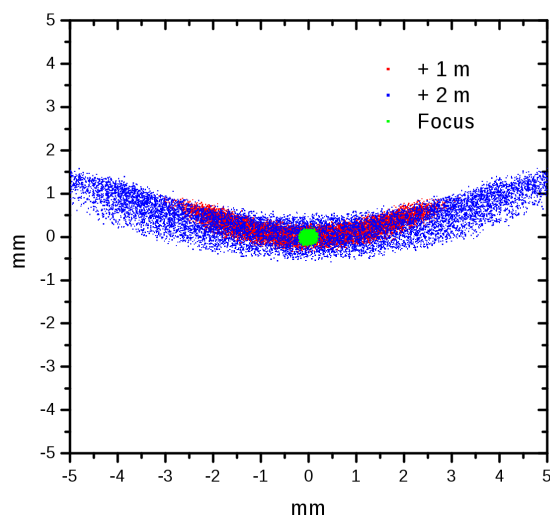


Figure 4: The shape of the focal spot at different positions in the experimental hutch.

4.1 Monochromatic beam

In normal operation the beamline employs the Si monochromator and both mirrors M1 and M2. This can be used for a wide range of experiments providing a monochromatic, tunable x-ray beam horizontally and vertically focused on the sample position. A spatial resolution of about $150\ \mu\text{m}$ can be achieved in this way over the whole energy range. Energy resolution is $\Delta\lambda/\lambda \approx 4525\text{--}5000$ depending on the energy (Fig. 2).

4.2 White Beam

In this configuration only the mirror system without the monochromator are in the optical path. The first monochromator crystal is vertically translated out of the beam and M2 is lowered 25 mm to receive the white beam. The exit window, as well as the experimental setup must be manually lowered 25 mm to accommodate the white beam. The energy spectra of the beamline in two modes are shown in the figure 3.

Filter	differentially pumped Capton/Be windows. (Pos. 30 000 mm, experimental hutch). Thickness: Capton: $25\ \mu\text{m}$, Be $200\ \mu\text{m}$
premonochromator optics	Paraboloid of rotation Si / Pt 60nm + Rh 5nm optical surface size: $1200 \times 60\ \text{mm}^2$, $\theta = 0.3^\circ$
Monochromator	Double-crystal monochromator, angular range $-3^\circ - 80^\circ$ Crystals: Si (111) $30 \times 70\ \text{mm}^2$ 10 mm thick
Refocusing optics	Paraboloid of rotation Si Pt 60 nm + Rh 5 nm optical surface size: $1200 \times 60\ \text{mm}^2$, $\theta = 0.3^\circ$
Diagnostics	Ionisation chamber for MOSTAB intensity control and feedback Standard Screen Monitor for beam profiling
Slits	Four-blades slit system S2, not water cooled. (Pos. 23 000 mm) two vertical independent tungsten blades, motorized feedthrough. Maximum aperture: $60\ \text{mm} \times 20\ \text{mm}$ Step size $10\ \mu\text{m}$

Table 2: Optical components and parameters of the KMC-3 beamline.

5 Technical Data

The beamline is built in Ultra-High-Vacuum windowless technique separated from the experiment by 150 μm thick beryllium window. The optical concept incorporates two focusing/refocusing options, which can be used alternatively to provide a large flexibility in terms of desired focal size, energy resolution (Fig. 2) and photon flux (Fig. 3) for different experiments.

Depending on the flux requirements, experiments can be mounted in focus or at the distance between 1 m and 2 m behind the focus. Permanent diffraction XPP experiment is mounted in focus to match the focus of the pumping laser. CryoEXAFS experiment is mounted 2 m behind the focus to avoid the radiation damages. Figure 4 shows the beam cross section at different distances from the focal spot.

Segment	H13
Location (Pillar)	15.1
Source	D 13.2
Monochromator	KMC-3 (FMB Oxford)
Energy range	2.2 - 14 keV
Energy resolution	1/1000 - 1/5000
Flux	$\sim 1 \times 10^{11}$ photons/s (see Fig. 3)
Polarisation	horizontal
Divergence horizontal	300 mrad
Divergence vertical	0.3 mrad
Focus size (<i>hor.</i> \times <i>vert.</i>)	250 μm \times 120 μm
Distance focus - last valve	200 mm
Height Focus over floor level	1500 mm
Free photon beam	available
Fixed end station	two alternating stations
Beam available	24 h/d 6 days/week
Phone	+49 30 8062 14695

Table 3: Technical data of the KMC-3 beamline.

References

- Görlin, M., Chernev, P., Ferreira de Araújo, J., Reier, T., Dresch, S., Paul, B., ... Strasser, P. (2016). Oxygen Evolution Reaction Dynamics, Faradaic Charge Efficiency, and the Active Metal Redox States of Ni-Fe Oxide Water Splitting Electrocatalysts. *Journal of the American Chemical Society*, 138(17), 5603-5614. <http://dx.doi.org/10.1021/jacs.6b00332>
- Helmholtz-Zentrum Berlin für Materialien und Energie. (2016). XPP: X-ray pump probe station at BESSY II. *Journal of large-scale research facilities*, 2, A89. <http://dx.doi.org/10.17815/jlsrf-2-82>
- Iurchuk, V., Schick, D., Bran, J., Colson, D., Forget, A., Halley, D., ... Kundys, B. (2016, Sep). Optical writing of magnetic properties by remanent photostriction. *Phys. Rev. Lett.*, 117, 107403. <http://dx.doi.org/10.1103/PhysRevLett.117.107403>
- Navirian, H. A., Schick, D., Gaal, P., Leitenberger, W., Shayduk, R., & Bargheer, M. (2014). Thermoelastic study of nanolayered structures using time-resolved X-ray diffraction at high repetition rate. *Applied Physics Letters*, 104(2), 021906. <http://dx.doi.org/10.1063/1.4861873>
- Roshchupkin, D., Ortega, L., Plotitsyna, O., Erko, A., Zizak, I., Vadilonga, S., ... Leitenberger, W. (2016). Piezoelectric $\text{Ca}_3\text{NbGa}_3\text{Si}_2\text{O}_{14}$ crystal: crystal growth, piezoelectric and acoustic properties. *Applied Physics A*, 122(8), 753. <http://dx.doi.org/10.1007/s00339-016-0279-1>



- Vadilonga, S., Zizak, I., Roshchupkin, D., Evgenii, E., Petsiuk, A., Leitenberger, W., & Erko, A. (2017). Observation of sagittal X-ray diffraction by surface acoustic waves in Bragg geometry. *Journal of Applied Crystallography*, 50(2), 525–530. <http://dx.doi.org/10.1107/S1600576717002977>
- Zaharieva, I., Gonzalez-Flores, D., Asfari, B., Pasquini, C., Mohammadi, M. R., Klingan, K., ... Dau, H. (2016). Water oxidation catalysis - role of redox and structural dynamics in biological photosynthesis and inorganic manganese oxides. *Energy Environ. Sci.*, 9, 2433-2443. <http://dx.doi.org/10.1039/C6EE01222A>